

1 Stable-isotope based location in a shelf sea setting: accuracy and precision are  
2 comparable to light-based location methods.

3

4 Clive N. Trueman<sup>1</sup>, Kirsteen M. MacKenzie<sup>1,2</sup>, Katie St John Glew<sup>1</sup>

5

6 Running title: Stable isotope-based location in shelf seas

7

8 Word count: 6986

9 Ocean and Earth Science, University of Southampton Waterfront Campus,

10 Southampton SO143ZH

11 Institute for Marine Research, Tromsø, Norway

12 CN Trueman: email [Trueman@noc.soton.ac.uk](mailto:Trueman@noc.soton.ac.uk)

13

14

15 1. Retrospective determination of location for marine animals would facilitate  
16 investigations of migration, connectivity and food provenance. Predictable  
17 spatial variations in carbon and nitrogen isotopes in primary production across  
18 shelf seas provide a basis for stable isotope-based location.

19

20 2. Here we assess the accuracy and precision that can be obtained through  
21 dietary-isotope based location methods. We build isoscapes from jellyfish tissues  
22 and use these to assign scallops of fixed and known individual location, and  
23 herring with well-understood population-level distributions in the North Sea.

24

25 3. Accuracy and precision for retrospective isotope-based location in the North  
26 Sea was of a similar order to light-based location devices, with 75% of individual  
27 scallops assigned correctly to areas representing c.30% of the North Sea, with a  
28 mean linear error on the order of  $10^2$ km. Applying assignment methods to an  
29 alternative migratory species (herring) resulted in ecologically realistic  
30 assignments consistent with fisheries survey data.

31

32 4. Location methods based on dietary isotopes such as carbon and nitrogen  
33 recover the spatial origin of nutrients assimilated into tissues and this may not  
34 correspond directly to the physical location if either the test animal or its prey is  
35 highly migratory. Stable isotope based location can be applied to any marine-  
36 feeding organism or derived food product, but the ecological meaning of any  
37 assigned area will be more difficult to interpret for large, high trophic level,  
38 migratory animals with relatively slow isotopic assimilation rates.

39

40 **Key-words:** Isoscape, assignment, provenance, connectivity, migration, spatial,

41 marine, geolocation

42

43

#### 44 **Introduction**

45 Understanding animal movements is fundamental to population dynamics,  
46 predator-prey relationships, nutrient and energy fluxes within food webs and  
47 management of human-animal interactions. In comparison to terrestrial animals,  
48 marine (and aerial) animals encounter relatively few static, physical barriers to  
49 movement and dispersal over areas large in comparison to body sizes is a  
50 common phenomenon. In the context of marine fisheries, mislabelling of fishery  
51 products has emerged as a major problem on global markets (Marko *et al.* 2004;  
52 Wong and Hanner, 2008; Nielsen *et al.* 2012, Cawthorn *et al.* 2012). Tracing  
53 marine food from origin to sale is a key aim of regulatory organisations  
54 worldwide. At present there are few effective retrospective analytical methods  
55 available to test claims of spatial origin of traded seafood.

56 Marine spatial ecology is undergoing a revolution with rapid  
57 developments in telemetry and electronic tagging technology with the  
58 deployment of large static acoustic arrays, satellite geo-location and the  
59 development of ever smaller less invasive data storage tags (Hunter *et al.* 2003;  
60 Righton *et al.* 2007; Block *et al.* 2011). Nonetheless, direct tagging of marine  
61 animals still requires capture and recovery of tags, and processing of data, and is  
62 relatively costly (Ramos & Gonzalez-Solis 2012). Furthermore, while tagging  
63 experiments reveal individual movements in high resolution, by definition, they  
64 cannot be applied retrospectively. Natural tags provide an attractive supplement  
65 to direct location tools. Natural location methods typically attempt to link the  
66 chemical (or parasite) composition of the test animal's tissues to known spatial  
67 variations in the environment (Hobson 1999, Graham *et al.* 2010, Seminoff *et al.*

68 2012, McMahon *et al.* 2013). In recent years, stable isotope location has proven  
69 effective at reconstructing long-distance migrations in terrestrial, particularly  
70 avian, ecology (Rubenstein & Hobson 2004; Wunder and Norris 2008; Hobson *et*  
71 *al.* 2012). Statistical models of spatial variation in the isotopic composition of  
72 precipitation (Bowen, 2010), vegetation (West *et al.* 2007; Still & Powell 2010, )  
73 and higher taxa tissue (Vander Zanden *et al.* 2015) have been developed in many  
74 environments and termed isoscapes. Such isoscapes can provide a base model to  
75 assign geographic origin to a tissue of interest, following calibration between the  
76 media used to construct the isoscape and the species and tissue to be assigned  
77 (Wunder & Norris 2008). A relatively mature literature has developed describing  
78 the construction of isoscapes, the statistical considerations surrounding  
79 geographic assignment based on isoscapes, and application of isoscapes to track  
80 animal movements (West *et al.* 2010).

81 Isotope-based location comprises a geo-statistical spatial model, a  
82 calibration between the model and the species and tissue to be assigned, and a  
83 probabilistic comparison between model and measured data. Isoscapes derived  
84 from the same species and tissues as those that will be assigned in theory  
85 provide the most robust method of assignment. However, the practical and  
86 financial limitations associated with sampling and analysing tissues of each  
87 migratory species across the full potential foraging range are considerable.  
88 Therefore the potential for isotope-based geo-location is greatly increased if  
89 multiple taxa can be referred to a single isoscape model. The accuracy and  
90 precision available for isotope-based location therefore depends on the variance  
91 associated with the underlying geostatistical isoscape model, *in situ* variability in  
92 the isotopic compositions of both the organism used to construct the model and

93 in the tissues to be assigned, and the uncertainty inherent in linking the isotopic  
94 compositions of the tissues to be assigned to the baseline isoscape (i.e.  
95 calibration of the isoscape to the tissue of interest, Wunder & Norris 2008).  
96 Considerable debate remains around the most effective way to incorporate error  
97 and uncertainty into stable isotope-based geographic assignment methods  
98 (Wunder & Norris, 2008; Van Wilgenburg *et al.* 2011; Wunder 2012; Bowen *et*  
99 *al.* 2014, Vander Zanden *et al.* 2015). Wunder (2008) provides a thorough review  
100 of the assumptions inherent in isotope-based location, focussing on hydrogen  
101 and oxygen isotope based geo-assignment specifically in migratory birds.

102

103         Isotope-based location is not as well developed in marine settings and  
104 very few robust assessments of the accuracy and precision obtained using  
105 isotope based location have been developed in marine settings (Vander Zanden  
106 *et al.* 2015). In marine systems oxygen and hydrogen isotopes are relatively  
107 spatially constant, so alternative isotope systems are needed to provide spatial  
108 information (Trueman *et al.* 2012). The isotopic composition of carbon and  
109 nitrogen in marine primary production is predictably heterogenous over spatial  
110 scales ranging from tens to thousands of kilometres (Jennings and Warr, 2003;  
111 Somes *et al.* 2010; McMahon *et al.* 2013; Radabaugh *et al.* 2013, Jennings & van  
112 der Molen 2015), and is passed through the food chain. Assigning location based  
113 on carbon and nitrogen isotopic compositions therefore effectively tracks the  
114 spatial origin of primary production fuelling higher trophic level production  
115 rather than the direct spatial location of the animal tested. Nonetheless carbon  
116 and nitrogen isotopes have been used extensively to track animal movements

117 across marine isotopic gradients (Hobsen & Schell, 1998; Jaegar *et al.* 2010,  
118 MacKenzie *et al.* 2012).

119 Marine carbon and nitrogen isoscape models are generated by  
120 interpolation from spatially explicit samples (Schell *et al.* 1998; McMahon *et al.*  
121 2013). Sessile invertebrates such as filter feeding bivalves have often been used  
122 to produce spatial isotope models (e.g. Jennings & Warr, 2003). However, the  
123 distribution of sessile invertebrates is limited by water depth and substrate type  
124 resulting in systematic variance in spatial coverage of reference samples across  
125 the study region. Environmental correlates such as water temperature, depth  
126 and salinity have been used to predict isotopic compositions in areas with no  
127 reference samples (Jennings & Warr 2003; Barnes *et al.* 2009; MacKenzie *et al.*  
128 2014), but the resulting isoscape models are strongly dependent on the location  
129 of the reference samples and the assumption that regression relationships  
130 between environmental drivers and isotope values derived in the sampled  
131 region are constant throughout the wider study area. The uncertainty associated  
132 with any predicted isotope value increases with (a) the error associated with the  
133 regression model, (b) the spatial distance from the reference sites and (c)  
134 isotopic or environmental differences between conditions at the predicted site  
135 and the mean of the combined reference sites. Estimating the spatially varying  
136 uncertainty associated with regression-based isoscape models is not trivial  
137 (Bowen & Ravenaugh 2003), and has not been attempted for marine isoscapes.  
138 An alternative approach lies in selecting pelagic reference organisms that are  
139 widely distributed, but may have larger between-individual variance associated  
140 with movement or diet ecology. Scyphomedusan jellyfish provide an attractive  
141 potential target due to their ubiquitous distributions, rapid growth and short

142 lifespans (MacKenzie et al 2014). While scyphomedusan jellyfish are mobile,  
143 movement is relatively passive and isotopic assimilation rates are fast. The  
144 isotopic half-life for the moon jellyfish *Aurelia aurita*, for example, is estimated at  
145 c.10 days (D'Ambra et al. 2014). The distance travelled by jellyfish during the  
146 window of isotopic assimilation is therefore likely to be short compared to the  
147 spatial scales of isotopic variance in open waters. Jellyfish may be a poor choice  
148 for spatial isotope modelling in coastal areas where isotopic variability occurs at  
149 smaller spatial scales.

150         Here we assess the precision and accuracy associated with using spatial  
151 gradients in carbon and nitrogen isotopes to assign origin to animal tissues  
152 across a relatively large shelf sea area. We derive carbon and nitrogen isoscapes  
153 from lion's mane jellyfish *Cyanea capillata* expanding on the dataset and  
154 methods outlined in (MacKenzie *et al.* 2014, Fig. 1). The North Sea is a shallow  
155 semi-restricted shelf sea in the North Atlantic ocean with a total area of around  
156 650,000km<sup>2</sup>, sustaining one of the productive fisheries in the world. The North  
157 Sea comprises a seasonally-stratified northern basin with a mean depth >50m,  
158 and a shallower southern basin that is not stratified. In this study we quantify  
159 the accuracy and precision associated with isotope-based geo-location in the  
160 North Sea using two independently-determined datasets of stable isotope  
161 compositions of the sessile queen scallop *Aequipecten opercularis* (Jennings *et al.*  
162 2002, Jennings & van der Molen, 2015). We then identify feeding locations of 351  
163 herring *Clupea harengus* caught at known locations throughout the North Sea.

164

## 165 **Materials and methods**

166

167 STABLE ISOTOPE SAMPLES

168

169 Following methods described in MacKenzie *et al.* (2014), 66 individuals of *C.*  
170 *capillata* were sampled from 52 stations in the North Sea in August 2015 during  
171 the International Bottom Trawl Survey on board the RV Cefas Endeavor. Jellyfish  
172 were collected, weighed and measured, and a section of bell tissue (mesoglea)  
173 removed and immediately frozen. Jellyfish ranged in size from 80 to 240mm in  
174 diameter (mean = 107mm,  $\sigma = 3.25$ mm). In the laboratory, tissues were washed  
175 3 times with water to remove any soluble nitrogenous materials, re-frozen prior  
176 to freeze-drying, sub-sampling and submission for isotopic analyses. Capture  
177 locations, body sizes and isotope data for jellyfish tissues are reported in Table  
178 S1 and locations are illustrated in Fig. 1.

179

180 351 individual herring were captured at 41 known locations within the North  
181 Sea during September 2011 as part of the International Bottom Trawling Survey.  
182 Fishing was conducted from the R.V. "Cefas Endeavor". After capture, herring  
183 were weighed, dorsal muscle was excised and frozen prior to analysis. Herring  
184 under 200mm standard length were grouped as 'small' fish, likely to represent  
185 juveniles, whereas fish greater than 200mm standard length are likely to be  
186 mature (ICES, 2012). Muscle samples were freeze dried, ground to a powder and  
187 analysed for carbon and nitrogen isotopic composition. Capture locations, body  
188 sizes and isotope data for herring muscle are reported in Table S2 and locations  
189 are illustrated in Fig. 2.

190

191 Analyses were performed by either OEA laboratories or Elementex laboratories,  
192 Cornwall, UK. Accuracy and precision were monitored through laboratory  
193 internal standards (USGS 40 and USGS 41 and a bovine liver standard) and  
194 repeat blind analyses of an in-house comparison standard (ARCOS glutamic acid)  
195 nested within samples. Accuracy in both laboratories for  $\delta^{13}\text{C}$  and  $\delta^{15}\text{N}$  values  
196 was within 0.1‰ of long-term average values for this standard, and precision  
197 was 0.2‰ for  $\delta^{13}\text{C}$  and 0.17‰  $\delta^{15}\text{N}$  values.

198 Jellyfish bell tissue  $\delta^{13}\text{C}$  values showed a significant negative linear  
199 relationship with C:N ratios ( $p = 4.54\text{e-}05$ , slope = -0.047, Adjusted  $R^2 = 0.2$ ),  
200 implying a variance component related to the concentration of isotopically light  
201 lipids within the sample. To correct for potential lipid-related variance in  $\delta^{13}\text{C}$   
202 values, measured  $\delta^{13}\text{C}$  values were adjusted to those predicted for a lipid-free  
203 protein (atomic C:N ratio of 3.4) using linear regression between  $\delta^{13}\text{C}$  values and  
204 C:N ratios. We did not apply alternative arithmetic lipid correction terms as the  
205 measured C:N ratios are close to those expected from pure protein with a small  
206 range (mean = 3.6,  $\sigma = 0.15$ ) implying that linear corrections are equally  
207 effective (Kiljunen *et al.* 2006), and we therefore prefer to use correction terms  
208 derived from the species and individuals studied. Lipid-corrected  $\delta^{13}\text{C}$  values of  
209 jellyfish show a positive correlation with bell diameter, accordingly they were  
210 normalised to the median diameter (107mm):

211

$$212 \delta^{13}\text{C}_{\text{s.cor}} = \delta^{13}\text{C}_{\text{cor}} + (\text{Diameter} - 10.73) * 0.19 \quad \text{eqn 1}$$

213

214 Herring muscle contained varying C:N ratios, and  $\delta^{13}\text{C}$  values were corrected for  
215 lipid content arithmetically (Kiljunen et al. 2006).

216

217 Isotopic data from queen scallops was recovered from Jennings & Warr  
218 (2003) and Barnes *et al.* (2009) for scallops sampled between 25 July and 29  
219 September 2001, and from S. Jennings (*pers. comm.* 2016) for scallops sampled in  
220 similar locations in the summer of 2010 (Jennings & van der Molen, 2015). Up to  
221 seven individual scallops were sampled in each area. Locations of capture sites  
222 are shown in Fig. 2, Details of sampling, preparation and analytical  
223 methodologies are provided in Jennings & Warr (2003), Barnes *et al.* (2009) and  
224 Jennings & van der Molen, 2015.

225

## 226 STATISTICAL ASSIGNMENT METHODS

227

228 Statistical models of spatial variation in the isotopic composition of carbon and  
229 nitrogen in jellyfish tissues sampled in 2015 were drawn from the lipid and size-  
230 corrected isotope data using Linear Kriging. Isoscapes are presented in Fig. 1  
231 together with the associated spatial variances, and locations of jellyfish sampled  
232 to create the isoscapes. Raster files of the isoscape values are provided as  
233 supplementary data.

234

235 In isotope-based Geo-assignment, the likelihood or probability of the sample  
236 originating from a given location or cell in the isoscape depends on the isotopic  
237 difference between the sample and cell value relative to the total variance in the  
238 isoscape. As described above, much of the difficulty associated with isotope-

239 based location lies in quantifying sources of variance, a problem that is  
240 particularly acute when using environmental correlates to extend predictions  
241 into regions with no reference samples.

242 As our isoscape model does not contain values predicted from regression  
243 models, variance associated with the isoscape is composed of a spatially varying  
244 term related only to the physical distance between sample points estimated from  
245 the kriging process, and a fixed term reflecting measurement error and between-  
246 individual variance (Bowen *et al.* 2014). Measurement error associated with  
247 jellyfish analyses determined as the standard deviation from 13 replicate  
248 analyses of the glutamic acid standard was 0.2‰ for  $\delta^{15}\text{N}$  and 0.1‰ for  $\delta^{13}\text{C}$   
249 analyses. Between-individual variances in jellyfish isotope compositions were  
250 estimated from jellyfish sampled both in 2011 (MacKenzie *et al.* 2014) and in  
251 2015 as 1.69‰ and 1.04‰ for  $\delta^{13}\text{C}_{\text{cor}}$  and  $\delta^{15}\text{N}$  values respectively. These  
252 between-individual variance estimates are similar to those provided for  
253 gelatinous zooplankton by Nagata *et al.*, (2015) and Fleming *et al.*, (2015),  
254 particularly when accounting for the marked effect of size on isotopic variance in  
255 the Fleming *et al.* (2015) data. Total uncertainty in the assignment isoscape was  
256 given by:

257

$$258 \quad \sigma^2_{\text{iso}(x,y)} = \sigma^2_{\text{k.iso}(x,y)} + \sigma^2_{\text{m.iso}(x,y)} + \sigma^2_{\text{bi.iso}(x,y)} \quad \text{eqn 2}$$

259

260 where  $\sigma^2_{\text{iso}(x,y)}$  is the pooled variance associated with the isoscape prediction,

261  $\sigma^2_{\text{k.iso}(x,y)}$  is the variance associated with the spatial interpolation model,  $\sigma^2_{\text{m.iso}}$

262  $\sigma^2_{(x,y)}$  is the variance associated with measurement error and  $\sigma^2_{bi.iso (x,y)}$  is the  
263 variance associated with *in situ* between-individual variation.

264 Measurement error associated with  $\delta^{15}N$  analyses of scallop tissues was  
265  $<0.2\text{‰}$ , and the mean standard deviation between individual scallops was  
266  $0.8\text{‰}$ , similar to between-individual variance in *C. capillata*  $\delta^{15}N$  values  
267 (Jennings & Warr 2003, Jennings & van der Molen 2015). We estimate associated  
268 measurement precision associated with  $\delta^{13}C$  values in scallop tissues as  $0.2\text{‰}$ ,  
269 similar to measurement errors associated with  $\delta^{13}C$  analyses of *C capillata*.  
270 Between-individual variance in lipid-corrected  $\delta^{13}C$  values of scallops across 22  
271 stations sampled in 2010 was  $0.21\text{‰}$  (Jennings *pers. comm.* 2016).

272 Pooled error associated with the measurement of scallop stable isotope  
273 compositions is therefore given by:

274

$$275 \sigma^2_{assign (x,y)} = \sigma^2_{m.assign (x,y)} + \sigma^2_{bi.assign (x,y)} \quad \text{eqn 3}$$

276

277 where  $\sigma^2_{assign (x,y)}$  is the pooled variance associated with the isoscape prediction,  
278  $\sigma^2_{m.assign (x,y)}$  is the variance associated with measurement error and  $\sigma^2_{bi.assign (x,y)}$   
279 is the variance associated with *in situ* between individual variation.

280 Uncertainties associated with calibration between the isoscape model and  
281 the tissue to be assigned were estimated from the combined uncertainty  
282 associated with trophic separation and trophic fractionation between jellyfish  
283 and scallops (e.g Wunder & Norris 2008). Trophic separation between jellyfish  
284 and scallops was constrained from known diet preferences. Scallops are filter-  
285 feeding molluscs sustained primarily on detrital phytoplankton and

286 microzooplankton. Lion's mane jellyfish are opportunistic pelagic predators  
287 consuming a range of macro-zooplankton and larval/juvenile fish. The jellyfish  
288 sampled in 2015 encompassed a relatively narrow size range from 80 to 240mm  
289 bell diameter equivalent to a wet mass of c. 100-500g, and no systematic size-  
290 related difference in trophic level between sampled individuals is expected  
291 (Fleming *et al.*, 2015). Mass balance (Ecopath) modelling of the North Sea  
292 community (Mackinson & Daskalov, 2007) estimates scallop and gelatinous  
293 zooplankton trophic levels as 2.8 and 3.6 respectively. We therefore estimate the  
294 trophic distance between *C. capillata* and *A. opercularis*, as a single trophic level  
295 and assign uncertainty to that estimate with standard deviation of 0.25, ensuring  
296 that 95% of the estimates of trophic distance between scallops and *C. capillata*  
297 fall between 0.5 and 1.5 trophic levels.

298         Isotopic fractionation between tissue and diet (trophic fractionation) is  
299 estimated as 3.4‰ for nitrogen and 1‰ for carbon (Vander Zanden &  
300 Rasmussen, 2001) with a standard deviation of 0.5‰ ensuring that 95% of the  
301 estimates of isotopic trophic fractionation fall between 2.4 and 4.4‰ for  
302 nitrogen and between 0 and 2‰ for carbon. We then created 10,000 trophic  
303 fractionation and trophic distance values drawn from the distributions described  
304 above and estimated the distribution of isotopic separation values between  
305 jellyfish and scallops.

306         Scallop muscle and jellyfish bell tissue have contrasting biochemical  
307 compositions and therefore have potential for additional isotopic offsets. We do  
308 not know of any studies reporting isotopic discrimination between jellyfish bell  
309 tissue and coexisting muscle while accounting for trophic level. As all scallops  
310 are known to derive from the isoscape area, trophic-level corrected values

311 should lie within the total range of isotopic values within the isoscape. We  
312 therefore compare trophic level-corrected scallop data to the full range of  $\delta^{13}\text{C}$   
313 and  $\delta^{15}\text{N}$  values contained in the isoscape, and apply the smallest offset term  
314 required to ensure that all measured scallop values lie within the range  
315 described by the isoscape. For scallops we therefore apply an additional tissue-  
316 specific adjustment of +1‰ ( $\sigma = 0.5$ ) for  $\delta^{15}\text{N}$  and +0‰ ( $\sigma = 0.5$ ) for  $\delta^{13}\text{C}$  values.  
317 The final correction also accounts for any systematic under or over-estimation of  
318 trophic differences or isotopic fractionation. The estimated variance associated  
319 with calibration between scallop and jellyfish tissues  $\sigma^2_{\text{calib}}$  is therefore  
320 composed of the variance in estimated isotopic spacing across the 10,000 draws  
321 and the estimated variance around the remaining tissue calibration offset  
322

$$323 \quad \sigma^2_{\text{calib}(x,y)} = \sigma^2(\text{TD} * \text{TF}_{(x,y)}) + \sigma^2_{\text{off}(x,y)} \quad \text{eqn 4}$$

324  
325 where x and y refer to  $\delta^{13}\text{C}$  and  $\delta^{15}\text{N}$  values respectively, TD is the distribution of  
326 trophic difference values, TF is the distribution of isotopic fractionation values  
327 and  $\sigma^2_{\text{off}}$  is the estimated variance associated with the tissue offset.

328         We apply the method outlined above to quantify variance terms  
329 associated with assigning herring to the same *C. capillata*-defined isoscape.  
330 Herring are gape-limited zooplankton feeders with a similar diet and trophic  
331 level to predatory jellyfish. Ecopath modelling assigns herring a trophic level of  
332 3.4 and gelatinous zooplankton a trophic level of 3.6 (Mackinson & Daskalov  
333 2007). We therefore assign a trophic difference between herring and *C. capillata*  
334 of -0.5 with a standard deviation of 0.5. Multiple individuals were sampled in all

335 41 locations, and mean between-individual standard deviations were 0.44‰ for  
 336  $\delta^{15}\text{N}$  and 0.39‰ for lipid-corrected  $\delta^{13}\text{C}$  values. Minimum tissue offset values  
 337 between herring and jellyfish were estimated as described above as +2‰  
 338 ( $\sigma=0.5$ ) for  $\delta^{13}\text{C}$  and +0.5‰ ( $\sigma 0.5$ ) for  $\delta^{15}\text{N}$ . A summary of assignment  
 339 conditions is provided in Table 1.

340 We follow the assignment approach outlined in Vander Zanden et al.  
 341 2015:

$$f(x, y | \mu_i, \Sigma) = \frac{1}{\left(2\pi\sigma_x\sigma_y\sqrt{1-\rho^2}\right)} \times \exp\left(-\frac{1}{2(1-\rho^2)}\left[\frac{(x-\mu_x)^2}{\sigma_x^2} + \frac{(y-\mu_y)^2}{\sigma_y^2} + \frac{2\rho(x-\mu_x)(y-\mu_y)}{\sigma_x\sigma_y}\right]\right)$$

342 eqn 5

343

344 where  $f(x,y|\mu_i,\Sigma)$  represents the probability that an individual with adjusted  
 345 isotopic composition ( $\delta^{13}\text{C}=x$  and  $\delta^{15}\text{N}=y$ ) originates from a given cell (i) within  
 346 the isoscape with mean isotopic composition equal to the components of vector  
 347  $\mu_i$ , and variance co-variance matrix  $\Sigma$ .  $\rho$  is the correlation between  $\delta^{13}\text{C}$  and  $\delta^{15}\text{N}$   
 348 values throughout the isoscape,  $\sigma_x$  and  $\sigma_y$  are the pooled standard deviations in  
 349  $\delta^{13}\text{C}$  and  $\delta^{15}\text{N}$  values respectively given by the sum of the variances:

350

$$351 \sigma_{(x,y)} = \sqrt{\left(\sigma^2_{\text{iso}(x,y)} + \sigma^2_{\text{assign}(x,y)} + \sigma^2_{\text{off calib}(x,y)}\right)} \quad \text{eqn 6}$$

352

353 The range in pooled error terms across the isoscape for scallop assignment was  
354 3.5-12.4‰ for  $\delta^{13}\text{C}$  values and 5.5-11.6‰ for  $\delta^{15}\text{N}$  values, approximately three  
355 times higher than the pooled error estimates provided by Vander Zanden *et al.*  
356 (2015) where no calibration was needed between isoscape and assignment  
357 tissue.

358

#### 359 DISPLAYING ASSIGNMENT OUTCOMES

360

361 The outcome of stable-isotope based location can be displayed as continuous  
362 surfaces, but it is easier to describe accuracy and precision based on discrete  
363 assignments to a probable area defined by a probability threshold (i.e. an area  
364 containing all sites with an assignment probability higher than an arbitrarily  
365 fixed value). We use odds ratios to set threshold values (Van Wilgenburg *et al.*  
366 2012, Vander Zanden *et al.* 2015). The odds of an event occurring is given by the  
367 probability of the event occurring relative to the probability of that event not  
368 occurring (or  $P/1-P$ ). Thus a likely event has high odds. Here we define the odds  
369 *ratio* as the ratio of odds of the outcome occurring compared to the odds of the  
370 most likely outcome possible given the available data:

371

$$372 \text{Odds Ratio} = (P/1-P_i)/(P/1-P_{i.\text{max}}) \quad \text{eqn 7}$$

373

374 By setting an odds ratio threshold, all cells with probability values greater than  
375 the threshold are defined as cells of likely origin. The reciprocal of the odds ratio  
376 gives the total proportion of data (and thus the total proportional area) expected  
377 within the threshold limit according to the normal probability density function.

378 For instance, an odds ratio threshold of 2:1 includes all cells representing the  
379 most likely  $2^{-1} = 50\%$  of all data outcomes and defines a region of likely origin  
380 that is 50% of the total isoscape area. The precision of isotope-based assignment  
381 is thus defined by the odds ratio threshold, and the accuracy is given by the  
382 proportion of assigned individuals where the true location is contained within  
383 the assigned area (Vander Zanden *et al.* 2015).

384

## 385 **Results**

### 386 ISOSCAPES

387

388 The spatial isotope models (isoscapes) derived from *C. capillata* are shown in  
389 Fig. 1 A,B. Broad spatial patterns are similar to those shown in Jennings *et al.*  
390 2003; Barnes *et al.* 2009; MacKenzie *et al.* 2014 and Jennings & van der Molen  
391 2015, indicating consistent and temporally stable spatial isotopic gradients, and  
392 isotopic ranges that are conserved between pelagic and benthic feeding  
393 organisms. The newly derived isoscapes are drawn from samples with relatively  
394 regular spacing across the modelled area, and the variance associated with the  
395 new isoscape models is relatively low and constant across the region Fig 1 C,D.

396

### 397 ASSIGNMENT ACCURACY AND PRECISION

398

399 The accuracy associated with assigning a geographic origin to the two  
400 temporally distinct scallop tissue datasets considering uncertainties in  
401 calibration terms and between-individual variance is shown in Fig. 3. The  
402 assignment method provides better than random accuracy at all odds ratio

403 thresholds (Fig. 3). Assignments are >90% accurate when assigning to areas that  
404 on average represent >40% of the total area of the North Sea. Precision is  
405 enhanced at the expense of accuracy: Doubling the assignment precision to areas  
406 encompassing 20% of the total North Sea reduces accuracy to 50%. The mean  
407 linear error between the cell of maximum likelihood and the known location was  
408 226 ( $\sigma = 137$ ) km for the 2001 scallop data and 318 ( $\sigma = 114$ ) km for the 2010  
409 scallop data.

410

#### 411 HERRING ASSIGNMENT

412

413 Herring were assigned to likely feeding areas using the assignment parameters  
414 outlined in Table 1. To report pooled results, individual herring areas were  
415 grouped according to body size. Following Van Wilgenburg *et al.* (2011), for each  
416 fish, cells designated as likely feeding areas were assigned a value of 1 and all  
417 other cells assigned a value of 0. Values were then summed for each cell across  
418 the total number of individual fish and divided by the total number of fish,  
419 providing an index of the most frequently assigned cells ranging between 0 and 1  
420 (Fig. 4). Irrespective of capture location, larger fish are assigned to feeding areas  
421 in the central northern North Sea (Fig. 4A), consistent with summer fishery  
422 catches (ICES 2012, Fig. 4C). Smaller (juvenile) herring are assigned to feeding  
423 areas in the southern North Sea particularly around the German Bight (Fig. 4B),  
424 again consistent with locations of juvenile herring inferred from acoustic surveys  
425 (ICES 2012, Fig. 4D).

426

#### 427 **Discussion**

428

429 ISOTOPE-BASED LOCATION ACCURACY AND PRECISION

430

431 Despite combined uncertainties associated with measurement, between  
432 individual variance, and calibration between an isoscape and measured tissues,  
433 isotope-based location was 75% accurate to 30% of the North Sea, equivalent to  
434 a spatial precision on the order of  $10^5$  km<sup>2</sup>. The mean linear error between the  
435 single cell of highest probability and the known location was between 200 and  
436 300 km. Light-based location is widely used in animal ecology, but relatively few  
437 studies have tested accuracy of light based location. Where direct tests have been  
438 reported, mean errors of location by light range between around 200-400km  
439 (Phillips *et al.* 2004; Lisovski *et al.* 2012), approximately equivalent to linear  
440 errors reported here for isotope-based location methods.

441

442 The isoscape used here is derived from a mobile pelagic organism, but used to  
443 assign origin to a sessile benthic organism collected either 4 or 14 years prior to  
444 the samples used to derive the isoscape. This mismatch in sample collection time  
445 and organism functional group is deliberate, testing the degree to which  
446 isoscapes derived from a single reference organism can be used to assign a wide  
447 range of taxa over unspecified periods of time.

448

449 Short and long-term temporal variation in isotopic baselines could confound the  
450 use of isotopes for geolocation. Scallops have been sampled in 2001 and 2010,  
451 and jellyfish in 2011 (MacKenzie *et al.*, 2014) and 2015. The regional distribution  
452 of isotope values was consistent across these four independent sampling dates,

453 although the exact location of boundaries between isotopically distinct regions  
454 varies slightly between sample suites. Consequently assignment accuracy is  
455 relatively consistent between the two test datasets (Fig. 3). This is consistent  
456 with broad hydrological control over spatial distribution of isotope values,  
457 modified by relatively minor intra-year variability (MacKenzie *et al.*, 2014;  
458 Jennings & van der Molen 2015). While jellyfish mesoglea sample spring and  
459 summer production, scallops have a longer isotopic turnover times and likely  
460 integrate annual average production (Jennings & van der Molen 2015). The  
461 similarity between jellyfish and scallop isoscapes further supports the argument  
462 that spring and summer primary production dominates biomass-weighted  
463 consumer tissue production in this strongly seasonal sea. At higher spatial  
464 resolution, or in coastal settings, isotopic compositions of primary production  
465 and dissolved organic matter are expected to vary more widely in both time and  
466 space (Kürten *et al.* 2013), and the spatial isotope models presented here are  
467 unlikely to perform well.

468

#### 469 GEOGRAPHIC ASSIGNMENT OF MIGRATORY FISHES

470

471 Herring present a particular challenge for fishery management, as they exhibit  
472 complex migratory behaviour and variation in spawning strategies which change  
473 in response to environmental conditions, population sizes, age structures and  
474 harvesting (Dickey-Collas *et al.* 2010). North Sea herring feed in open waters in  
475 the northern North Sea in summer months, before migrating south and east to  
476 spawn in discrete locations dictated by the need for well-oxygenated coarse  
477 substrates. Larval herring drift eastwards within the southern North Sea

478 towards the German Bight before recruiting to the adult population. Isotope-  
479 based geo-assignment captures this ontogenetic migration (Fig. 4), implying that  
480 isotope based location offers a promising additional tool for marine spatial  
481 ecology and management.

482

#### 483 IMPLICATIONS FOR ECOLOGY, MANAGEMENT AND FOOD TRACEABILITY

484

485 Stable isotope-based retrospective location is well-established in terrestrial  
486 ecology, particularly for birds, but extension into marine environments has been  
487 slow due to the difficulty of obtaining baseline spatial isotope data. Here we  
488 show that isotopic baselines derived from carbon and nitrogen isotopic  
489 compositions of pelagic gelatinous zooplankton provide sufficient spatial  
490 resolution to rival light-based location in terms of accuracy and precision.

491         Determining location based on carbon and nitrogen isotope compositions  
492 records a fundamentally different ecological variable to other location methods.  
493 While data storage tag, satellite and water chemistry-based locations record the  
494 physical position of the animal, dietary isotope based locations record the likely  
495 spatial origin of nutrients assimilated during feeding. In sessile animals, or  
496 animals with a limited foraging range, feeding location and physical location will  
497 be effectively the same within the error of the assignment methods. In mobile  
498 animals (or animals feeding on mobile prey), however, assigned feeding location  
499 reflects the origin of primary production assimilated during feeding. Potentially,  
500 the location associated with assimilation of food may not necessarily correspond  
501 to the location where an animal spends the majority of its time.

502           Dietary isotope-based location provides additional ecological information  
503 beyond location at a fixed point in time, but interpreting the ecological meaning  
504 of dietary isotope 'location' in migratory animals requires some understanding  
505 of the timescale of isotopic assimilation relative to the rate and scale of  
506 movements across isotopic gradients. Herring are relatively small, metabolically-  
507 active, low trophic level (Mackinson & Daskalov 2007) fish, and isotopic  
508 equilibration is likely to occur with a half life on the order of c.50 days (Miller  
509 2000; vander Zanden et al 2015). Consequently, isotopic-assignment areas for  
510 herring closely correspond to feeding areas. Dietary isotope-based identification  
511 of feeding grounds will be more problematic in animals where isotopic  
512 assimilation rates are slow with respect to movements across isotopic gradients.  
513 While static physical location tags (e.g. light or tidal-stream based location) can  
514 provide an answer to the question of where animals go (Hammerschlag *et al.*  
515 2011), combinations of physical tags and isotopic location may go some way  
516 towards addressing questions of why animals spend time in particular regions.

517           The accuracy and precision of location methods based on carbon and  
518 nitrogen stable isotopes is highly dependent on the isotopic calibration between  
519 the baseline organism and the species and tissue to be assigned. Estimates of  
520 uncertainty associated with all steps in isotopic measurement, spatial modelling  
521 and calibration can be quantified and incorporated into assignment algorithms.  
522 Calibration methods and uncertainties must be reported with any stable isotope  
523 assignment. Nevertheless we suggest that stable isotope based geoassignment  
524 can be used in marine systems retrospectively to infer the location where the  
525 majority of nutrients were assimilated prior to capture. The method can in  
526 theory be applied to any marine feeding organism, but the ecological meaning of

527 any assigned area will be more difficult to interpret for high trophic level and

528 migratory animals with relatively slow isotopic assimilation rates.

529

530

531

532 **Acknowledgements**

533 Simon Jennings (Cefas) is gratefully thanked for access to scallop isotope data.  
534 Cefas staff and crew of the RV Cefas Endeavor kindly allowed KSG to participate  
535 in the 2015 IBTS survey. Mike Wunder, Hannah Vander Zanden, Steve Van  
536 Wilgenburg and staff of the ITCE Spatial course in Utah in 2015 are all thanked  
537 for informative and constructive discussions that shaped the analyses performed  
538 here. KSG is funded through the SPITFIRE NERC DTP partnership. The authors  
539 would also like to thank the editors and reviewers whose constructive comments  
540 improved the manuscript considerably.

541

542 **Data accessibility**

543 Jellyfish and herring isotope data and isoscape raster files are provided in the  
544 supplementary information. Stable isotope data from jellyfish, herring and  
545 previously published stable isotope data from Queen scallops sampled in 2001  
546 are also available from (doi:10.5061/dryad.609hp). Stable isotope data from  
547 queen scallops sampled in 2010 are available from Cefas. The owner of the data,  
548 Simon Jennings, will be archiving it in Dryad shortly. The final version of this  
549 manuscript will include a direct link to this data. If you are viewing the 'Accepted  
550 Articles' version after September 2016, please search 'North Sea stable isotope'  
551 with Simon Jennings as the author in Dryad to find the relevant data.

552

553 **References**

554 Barnes, C., Jennings, S. & Barry, J.T. (2009) Environmental correlates of large-  
555 scale spatial variation in the  $\delta^{13}\text{C}$  of marine animals. *Estuarine, Coastal and Shelf*  
556 *Science*, 81, 368-374.

557

558 Block, B.A., Jonsen, I.D., Jorgensen, S.J., Winship, A.J., Shaffer, A.J., Bograd, S.J.,  
559 Hazen, E.L., Foley, D.G., Breed, G.A., Harrison, A.L., Ganong, J.E., Swithenbank, A.,  
560 Castleton, M., Dewar, H., Mate, B.R., Shillger, G.L., Schaefer, K.M., Benson, S.R.,  
561 Weise, M.J., Henry, R.W. & Costa, D.P. (2011) Tracking apex marine predator  
562 movements in a dynamic ocean. *Nature*, 475, 86-90.

563

564 Bowen, G.J. & Ravenaugh J. (2003). Interpolating the isotopic composition of  
565 modern meteoric precipitation. *Water Resources Research*, 39, 1299, doi:  
566 10.1029/2003WR002086

567

568 Bowen, G.J. (2010) Isoscapes: Spatial pattern in isotopic biogeochemistry. *Annual*  
569 *Reviews in Earth and Planetary Science*, 38, 161-187.

570

571 Bowen, G.J., Liu, Z., Vander Zanden, H.B., Zhao, L. & Takahashi, G. (2014)  
572 Geographic assignment with stable isotopes in IsoMAP. *Methods in Ecology and*  
573 *Evolution*, 5, 201-206.

574

575 Cawthorn, D-M, Steinman, H-A. & Witthuhn, R.C. (2012) DNA barcoding reveals a  
576 high incidence of fish species misrepresentation and substitution on the South  
577 African market. *Food Research International*, 46, 30-40.

578

579 D'Ambra, I., Carmichael, R. & Graham, W. (2014) Determination of d13C and  
580 d15N and trophic fractionation in jellyfish: implications for food web ecology.  
581 *Marine Biology*, 161, 473-480.

582

583 Dickey-Collas, M., Nash, R.D.M., Brunel, T., van Damme, C.J.G., Marshall, C.T.,  
584 Payne, M.R., Corten, A., Geffen, A.J., Peck, M.A., Hatfield, E.M.C., Hintzen, N.T.,  
585 Enberg, K., Kell, L.T. & Simmonds, E.J. (2010) Lessons learned from stock  
586 collapse and recovery of North Sea herring: a review. *ICES Journal of Marine*  
587 *Science*, 67, 1875-1886

588

589 Graham, B.S., Koch, P.L., Newsome, S.D., McMahon, K.W. & Aurioles, D. (2010)  
590 Using isoscapes to trace the movements and foraging behavior of top predators  
591 in oceanic ecosystems. *Isoscapes: Understanding Movement, Pattern, and Process*  
592 *on Earth Through Isotope Mapping*. (eds J.B. West, G.J. Bowen, T.E. Dawson, & K.P.  
593 Tu), pp 299-318. Springer.

594

595 Hammerschlag, N., Gallagher, A.J. & Lazarre, D.M. (2011). A review of shark  
596 satellite tagging studies. *Journal of Experimental Marine Biology and Evolution*,  
597 398, 1-8.

598

599 Hobson, K.A. & Schell, D.M. (1998) Stable carbon and nitrogen isotope patterns  
600 in baleen from eastern Arctic bowhead whales (*Balaena mysticetus*). *Canadian*  
601 *Journal of Fisheries and Aquatic Science*, 55, 2601-2607.

602

603 Hobson, K.A., Atwell, L. & Wassenaar, L.I. (1999) Influence of drinking water and  
604 diet on the stable-hydrogen isotope ratios of animal tissues. *Proceedings of the*  
605 *National Academy of Sciences of the USA*, 96, 8003-8006.

606

607 Hobson, K.A., Van Wilgenburg, S.L. Wassenaar, L.I. & Larson, K. (2012) Linking  
608 hydrogen (d2H) isotopes in feathers and precipitation: Sources of variance and  
609 consequences for assignment to isoscapes. *PLOS One*, 7, e35137  
610

611 ICES (2012) Report of the Herring Assessment Working Group for the area south  
612 of 62N (HAWG), 13-22 March 2012, Copenhagen, Denmark. ICES CM  
613 2012/ACOM:06.  
614

615 Jaeger, A., Lecomte, V.J., Weimerskirch, H., Richard, P. & Cherel, Y. (2010) Seabird  
616 satellite tracking validates the use of latitudinal isoscapes to depict predators'  
617 foraging areas in the Southern Ocean. *Rapid Communications in Mass  
618 Spectrometry*, 24, 3456-3460  
619

620 Jennings, S., Greenstreet, S.P.R., Hill, L., Piet, G.J., Pinnegar, J.K., & Warr, K.J. (2002)  
621 Long-term trends in the trophic structure of the North Sea fish community:  
622 evidence from stable-isotope analysis, size-spectra and community metrics.  
623 *Marine Biology*, 141, 1085-1097.  
624

625 Jennings, S. & Warr, K.J. (2003) Environmental correlates of large-scale spatial  
626 variation in the  $\delta^{15}\text{N}$  of marine animals. *Marine Biology*, 142, 1131-1140.  
627

628 Jennings, S & van der Molen, J. (2015) Trophic levels of marine consumers from  
629 nitrogen stable isotope analysis: estimation and uncertainty. *ICES Journal of  
630 Marine Science* doi: 10.1093/icesjms/fsw120  
631

632 Kiljunen, M., Grey, J., Sinisalo, T., Harrod, C., Immonen, H. & Jones, R.I. (2006) A  
633 revised model for lipi-normalizing d13C values from aquatic organisms, with  
634 implications for isotope mixing models. *Journal of Applied Ecology*. 43, 1213-  
635 1222.

636

637 Kürten, B., Painting, S.J., Struck, U., Polunin, N.V.P. & Middleburg, J.J. (2013).  
638 Tracking seasonal changes in North Sea zooplankton trophic dynamics using  
639 stable isotopes. *Biogeochemistry*, 113: 167-187

640

641 Lisovski, S., Hewson, C.M., Klaassen, R.H.G., Korner-Nievergelt, F., Kristensen,  
642 M.W. & Hahn, S. (2012) Location by light: accuracy and precision affected by  
643 environmental factors. *Methods in Ecology and Evolution*, 3, 603-612

644

645 MacKenzie, K.M., Palmer, M.R., Moore, A., Ibbotsen, A.T., Beaumont, W.R.C.,  
646 Poulter, D.J.S. & Trueman, C.N. (2011). Locations of marine animals revealed by  
647 carbon isotopes. *Scientific Reports*, 1, 21, doi:10.1038/srep00021.

648

649 MacKenzie, K.M., Longmore, C., Preece, C., Lucas, C.H. & Trueman, C.N. (2014)  
650 Testing the long-term stability of marine isoscapes in shelf seas using jellyfish  
651 tissues. *Biogeochemistry*, 121, 441-454, doi 10.1007/s10533-014-0011-1

652

653 Mackinson, S. & Daskalov, G. (2007) An ecosystem model of the North Sea to  
654 support an ecosystem approach to fisheries management: description and  
655 parameterization. *Scientific Series Technical Reports, Cefas Lowestoft*, 142.

656

657 McMahon, K.W., Hamady, L-L. & Thorrold, S.R. (2013) A review of  
658 ecogeochemistry approaches to estimating movements of marine animals.  
659 *Limnology and Oceanography*, 58, 697-714.  
660

661 Marko, P.B., Lee, S.C., Rice, A.M., Gramling, J.L., Fitzhenry, T.M., McAlister, J.S.,  
662 Harper, G.R. & Moran, A.L. (2004). Mislabelling of a depleted reef fish. *Nature*,  
663 430, 309-310.  
664

665 Nielsen, E.E., Mac Aoidh, E., Maes, G.E., Milano, I., Ogden, R., Taylor, M., Hemmer-  
666 Hansen, J., Babbucci, M., Bargelloni, L., Bekkevold, D., Diopere, E., Grenfell, L.,  
667 Helyar, S., Limborg, M.T., Martinsohn, J.T., McEwing, R., Panitz, F., Patarnello, T.,  
668 Tinti, F., Van Houdt, J.K.J., Volckaert, F.A.M., Waples, R.S., FishPopTrace  
669 Consortium & Carvalho, G.R. (2012) Gene-associated markers provide tools for  
670 tackling illegal fishing and false eco-certification. *Nature Communications*, 3, 852.  
671 DOI:10.1038/ncomms1845.  
672

673 Phillips, R.A., Silk, J.R.D., Croxall, J.P., Afanasyev, V. & Briggs, D.R. (2004) Accuracy  
674 of location estimates for flying seabirds. *Marine Ecology Progress Series*, 266,  
675 265-272.  
676

677 Radaburgh, K.R., Hollander, D.J. & Peebles, E.B. (2013) Seasonal  $\delta^{13}\text{C}$  and  $\delta^{15}\text{N}$   
678 isoscapes of fish populations along a continental shelf trophic gradient.  
679 *Continental Shelf Research*, 68, 112-122.  
680

681 Ramos, R. & González-Solís, J. (2012) Trace me if you can: the use of intrinsic  
682 biogeochemical markers in marine top predators. *Frontiers in Ecology and*  
683 *Evolution*, 10, 258-266.

684

685 Righton, D., Quayle, V.A., Hetherington, S.H. & Burt, G. (2007) Movements and  
686 distribution of cod (*Gadus morhua*) in the southern North Sea and English  
687 Channel: results from conventional and electronic tagging experiments. *Journal*  
688 *of the Marine Biological Association of the UK*. 87, 599-613.

689

690 Rubenstein, D.R. & Hobson, K.A. (2004) From birds to butterflies: animal  
691 movement patterns and stable isotopes. *Trends in Ecology and Evolution*, 19,  
692 256-263.

693

694 Schell, D. M., Barnett, B.A. & Vinette, K.A. (1998). Carbon and nitrogen isotope  
695 ratios in zooplankton of the Bering, Chukchi and Beaufort seas. *Marine Ecology*  
696 *Progress Series*, 162, 11-23.

697

698 Seminoff, J.A., Benson, S.R., Arthur, K.E., Eguchi, T., Dutton, P.H., Tapilatu, R.F. &  
699 Popp, B.N. (2012). Stable isotope tracking of endangered sea turtles: Validation  
700 with satellite telemetry and delta N-15 analysis of amino acids. *PLOS One*, 7,  
701 e37403.

702

703 Somes, C.J., Schmittner, A., Galbraith, E.D., Lehmann, M.F., Altabet, M.A., Montoya,  
704 J.P., Letelier, R.M., Mix, A.C., Bourbonnais, A. & Eby, M. (2010) Simulating the

705 global distribution of nitrogen isotopes in the ocean. *Global Biogeochemical*  
706 *Cycles* 24, doi10.1029/2009GB003767.

707

708 Still, C.J. & Powell, R.L. (2010) Continental-scale distributions of vegetation stable  
709 carbon isotope ratios. (eds J.B. West, G.J. Bowen, T.E. Dawson, & K.P. Tu), pp179-  
710 193. *Isoscapes: Understanding Movement, Pattern, and Process on Earth Through*  
711 *Isotope Mapping*. Springer.

712

713 Trueman, C.N., MacKenzie, K.M. & Palmer, M.R. (2012) Identifying migrations in  
714 marine fishes through stable-isotope analysis. *Journal of Fish Biology* 81, 826-  
715 847.

716

717 Vander Zanden, M.J. & Rasmussen, J.B. (2001) Variation in  $\delta^{15}\text{N}$  and  $\delta^{13}\text{C}$  trophic  
718 fractionation: Implications for aquatic food web studies. *Limnology and*  
719 *Oceanography*, 46, 2061-2066

720

721 Vander Zanden H.B., Tucker, A.D., Hart, K.M., Lamont, M.M., Fujisaki, I., Addison,  
722 D.S., Mansfield, K.L., Phillips, K.F., Wunder, M.B., Bowen, G.J., Pajuelo, M., Bolten,  
723 A.B. & Bjorndal, K.A. (2015) Determining origin in a migratory marine  
724 vertebrate: a novel method to integrate stable isotopes and satellite tracking.  
725 *Ecological Applications* 25, 320-335.

726

727 Van Wilgenburg, S.L. & Hobson, K.A. (2011) Combining stable-isotope ( $\delta\text{D}$ ) and  
728 band recovery data to improve probabilistic assignment of migratory birds to  
729 origin. *Ecological Applications* 21, 1340-1351.

730

731 Van Wilgenburg, S.L., Hobson, K.A., Brewster, K.R. & Welker, J.M. (2012)

732 Assessing dispersal in threatened migratory birds using stable hydrogen isotope

733 ( $\delta D$ ) analysis of feathers. *Endangered Species Research*, 16, 17-29.

734

735 West, J.B., Ehleringer, J.R. & Cerling, T.E. (2007) Geography and vintage predicted

736 by a novel GIS model of wine delta O-18. *Journal of Agricultural and Food*

737 *Chemistry*, 55, 7075-7083.

738

739 West, J.B., Bowen, G.J. Dawson, T.E. & Tu, K.P. (eds) *Isoscapes: Understanding*

740 *Movement, Pattern, and Process on Earth Through Isotope Mapping*. Springer.

741

742 Wong, E. H-K & Hanner, R.H. (2008) DNA barcoding detects market substitution

743 in North American seafood. *Food Research International*, 41, 828-837.

744

745 Wunder, M.B. (2012) Determining geographic patterns of migration and

746 dispersal using stable isotopes in keratins. *Journal of Mammalogy*, 93, 360-367

747

748 Wunder, M.B. & Norris, D.R. (2008) Improves estimates of certainty in stable-

749 isotope-based methods for tracking migratory animals. *Ecological Applications*,

750 18, 549-559.

751

752

753 Supporting Information

754 Table S1. Locations of capture, bell diameter, bell weight and weight and stable  
755 isotope composition ( $\delta^{13}\text{C}$  and  $\delta^{15}\text{N}$ ) for *C capillata* recovered across the North  
756 Sea

757

758 Table S2. Locations of capture and stable isotope composition ( $\delta^{13}\text{C}$  and  $\delta^{15}\text{N}$ ) for  
759 *C harengus* recovered across the North Sea

760

761 C\_raster.gri, C\_raster.grd R-compatible raster files of the carbon isoscape model

762

763 N\_raster.gri, N\_raster.grd R-compatible raster files of the nitrogen isoscape

764 model

765

766 CVar\_raster.gri, CVar\_raster.grd R-compatible raster files of spatial variance in

767 the carbon isoscape model

768

769 NVar\_raster.gri, NVar\_raster.grd R-compatible raster files of spatial variance in

770 the nitrogen isoscape model

771

772

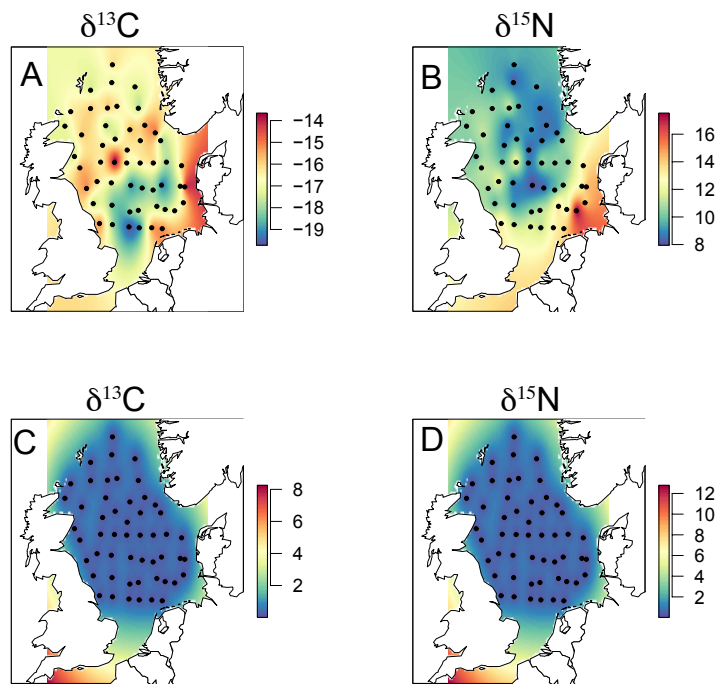
773 Table 1: Assignment conditions adopted for stable isotope based location of

774 scallops and herring against isoscapes derived from jellyfish tissues.

775

Variable	Isoscape jellyfish	Scallop calibration	Herring calibration
Measurement error	$\delta^{13}\text{C}$ : 0.1, $\delta^{15}\text{N}$ : 0.2:	$\delta^{13}\text{C}$ : 0.2, $\delta^{15}\text{N}$ : 0.2:	$\delta^{13}\text{C}$ : 0.2, $\delta^{15}\text{N}$ : 0.2:

( $\sigma$ )	measured	estimated / measured	measured
Between-individual variance	$\delta^{13}\text{C}$ : 1.69, $\delta^{15}\text{N}$ : 1.04: measured	$\delta^{13}\text{C}$ : 0.2, $\delta^{15}\text{N}$ : 0.7: estimated / measured	$\delta^{13}\text{C}$ : 0.2, $\delta^{15}\text{N}$ : 0.2: measured
Trophic distance	NA	1 ( $\sigma = 0.25$ ): literature estimate	-0.2 ( $\sigma = 0.25$ ): literature estimate
Isotopic trophic fractionation	NA	$\delta^{13}\text{C}$ : 1( $\sigma = 0.5$ ), $\delta^{15}\text{N}$ : 3.4( $\sigma = 0.5$ ): literature compilation	$\delta^{13}\text{C}$ : 1( $\sigma = 0.5$ ), $\delta^{15}\text{N}$ : 3.4( $\sigma = 0.5$ ): literature compilation
Tissue specific fractionation	NA	$\delta^{13}\text{C}$ : +0( $\sigma = 0.25$ ), $\delta^{15}\text{N}$ : +1( $\sigma = 0.25$ ): graphical estimate	$\delta^{13}\text{C}$ : +2( $\sigma = 0.25$ ), $\delta^{15}\text{N}$ : +0.5( $\sigma = 0.25$ ): graphical estimate
Threshold odds ratio	NA	1.33	1.5



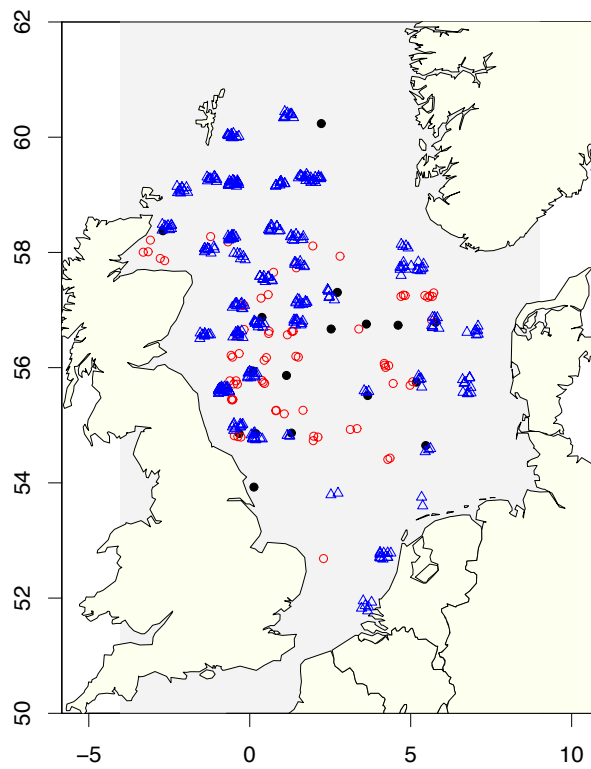
777

778 **Figure captions**

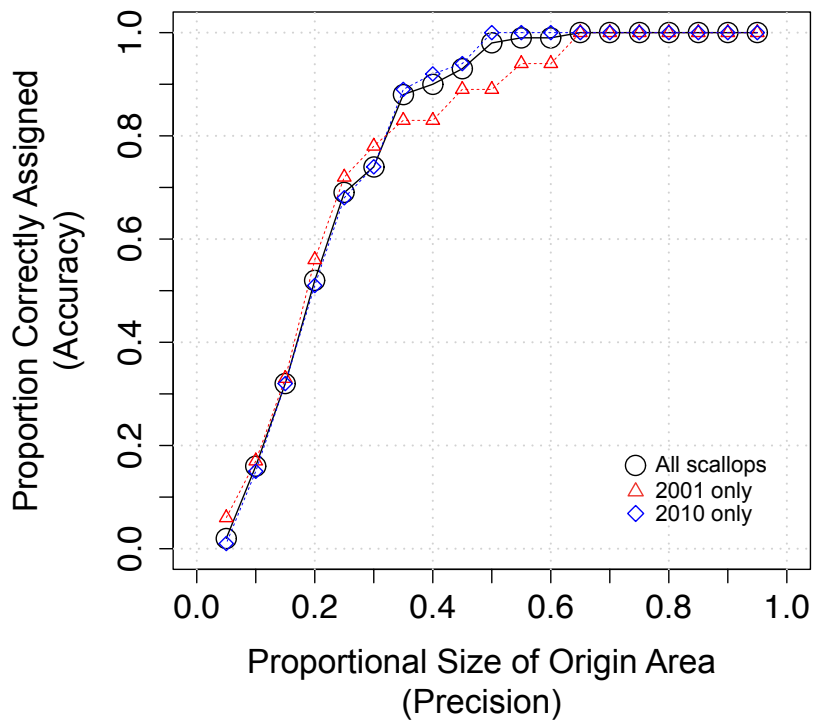
779

780

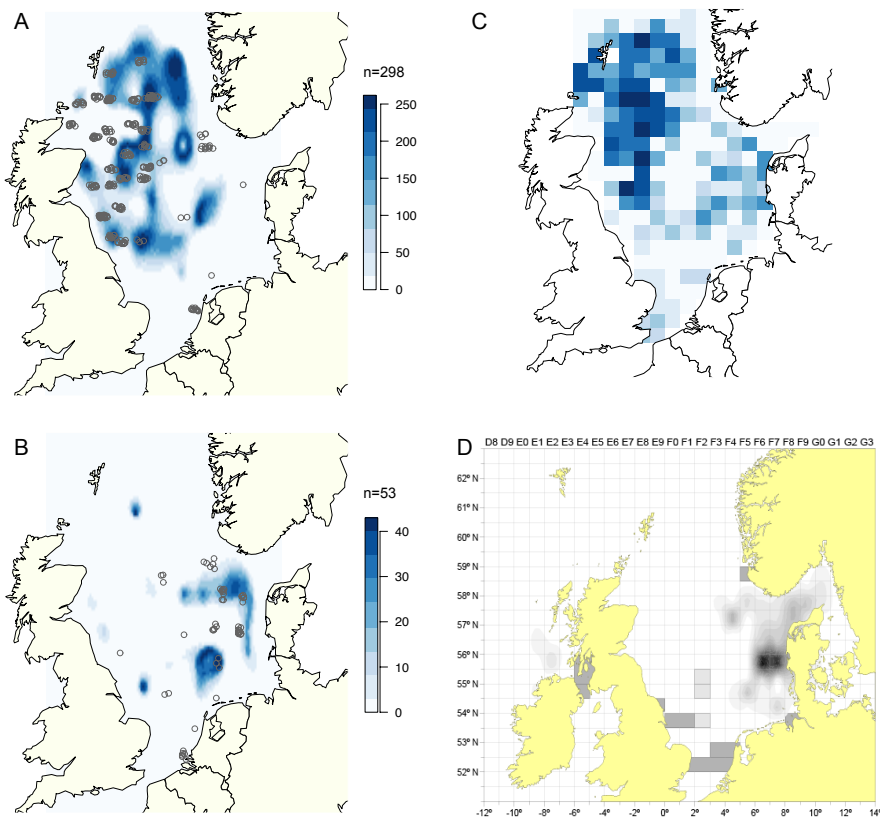
781 Fig. 1. Isoscape models (A, B) and associated variances (C,D) for  $\delta^{13}\text{C}$  (A, C) and  
782  $\delta^{15}\text{N}$  (B, D) values based on *C. capillata* sampled in September 2011. Sample  
783 stations indicated with filled circles.



785 Fig. 2 Locations of herring (open triangles) and scallop (2001 data: filled circles,  
786 2010 data: open circles) samples within the North Sea



788 Fig. 3 Accuracy and precision of assignment for the combined, 2001 and 2010  
789 scallop datasets. Precision is defined by the probability threshold and expressed  
790 as the proportion of data (i.e. cells) considered as likely. Accuracy is assessed as  
791 the proportion of individual scallops where the threshold area contained the  
792 known sample location.



793

794 Fig. 4. Comparison of isotope-based feeding area assignments and fisheries  
 795 survey data. A,B Most likely feeding areas for 351 North Sea herring sampled in  
 796 September 2011 as derived from stable isotope-based location. Colours

797 represent the number of individual herring assigned to each grid square. A)  
798 herring >200mm standard length, B herring <200mm standard length. Open  
799 circles indicate capture locations. C. Spatial distribution of reported landings of  
800 adult herring ( $\log_{10}$  tonnes) in quarters 2 and 3 of 2011, data from (ICES 2012).  
801 D. Estimated biomass of immature herring in June-July 2011 from combined  
802 acoustic surveys (ICES 2012).  
803  
804